

Total Variation Regularization in Digital Breast Tomosynthesis: Regularization Parameter Determination based on Small Structures Segmentation Rates

U. Heil*, S. Fränkel*[†], K. Wunder[†], D. Groß*, R. Schulze[‡], U. Schwanecke[§], C. Düber[†], E. Schömer*, and O. Weinheimer[†]

*Institute of Computer Science

Johannes Gutenberg-University Mainz (JGU), Staudingerweg 9, 55128 Mainz, Germany

Email: heilu@uni-mainz.de

[†]Department of Radiology, University Medical Center (UMC) of the JGU, 55131, Germany

[‡]Department of Oral Surgery (and Oral Radiology), UMC of the JGU, 55131, Germany

[§]Department of Design, Computer Science and Media, RheinMain University of Applied Sciences, 65197 Wiesbaden, Germany

Abstract—Regularization approaches for the limited-angle reconstruction problem in digital breast tomosynthesis are widely used. Though, their benefits depend largely upon a suitable regularization parameter estimation. We aim to evaluate the reconstruction quality of precise small contrast features objectively with the help of an automated process. These features were represented by so-called Landolt ring (LR) structures of descending sizes contained in an especially designed mammography test object (Quart Mam/Digi Phantom).

A GPU-based iterative Barzilai-Borwein (BB) algorithm is applied to solve the inverse reconstruction problem using total variation (TV) regularization. Exemplarily, we analyzed limited-angle breast projection images from a commercially available digital breast tomosynthesis (DBT) system (Siemens Mammomat Inspiration). We show that the TV regularization parameter and number of iterations can be chosen in such a way that the detection rate for the LR features is considerably higher than that obtained from the manufacturer’s reconstruction (modified filtered backprojection).

Index Terms—X-ray tomography, computed tomography, reconstruction algorithms, iterative algorithms, mammography, digital breast tomosynthesis, cone-beam geometry.

I. INTRODUCTION

Breast cancer remains a significant threat to woman’s health and the earlier the detection, the higher the chances for good healing prognoses. As tumor size at diagnosis is one of the main predictive factors for survival, all efforts are made to improve detection of small lesions. The 2D mammography is still the standard diagnostic method for screening and the diagnostic setting, although many studies showed limited sensitivity in dense breast tissue [1]. Now, that fast detectors and computers are available, standard tomography has been revitalized in breast diagnostics. In this technique, a 3D volume, respectively a stack of 2D slices, is computed by the use of a few projected X-ray images. The generated 3D information in digital breast tomosynthesis (DBT) should

improve lesion detection through reduction of superimposition. For reconstruction of the volume there are different algorithms like filtered back-projection (FBP), shift-and-add (SAA) or algebraic reconstruction techniques (ART). The results in [2] indicate that there may also be a substantial advantage in using TV regularization for microcalcification imaging. In [3] the influence of TV regularization on digital breast tomosynthesis data taken from a Hologic Selenia Dimensions system was analyzed.

In this paper, we investigate iterative image-reconstruction in DBT based on ART and TV with respect to detection of small clearly defined contrast features e.g. Landolt rings (LR) (see Fig. 1,2).

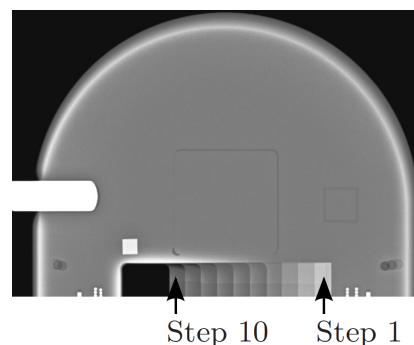


Fig. 1. 2D projection of the Quart Mam/Digi phantom. Step 11 and 12 are not displayed.

ART formulates the projection of a volume to images as the system of linear equations

$$\mathbf{Ax} = \mathbf{y}, \quad (1)$$

where $\mathbf{x} \in \mathbf{R}^n$ is an unknown 3D volume composed of n voxels written as a vector, $\mathbf{y} \in \mathbf{R}^{pm}$ is the set of p 2D images,

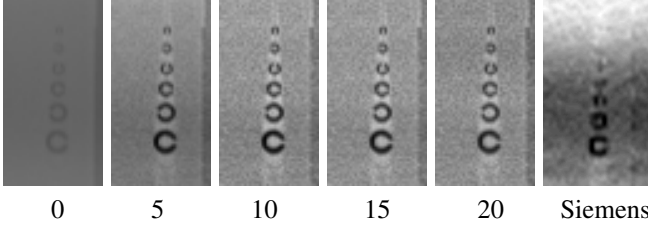


Fig. 2. A reconstructed Landolt ring sequence at one step of the Quart Mam/Digi phantom: six LRs at step 10, 200 mAs, 30 kVp, BB reconstruction, TV $\lambda = 0.2$, iterations 1 up to 20. On the right-hand side the corresponding Siemens Mammomat Inspiration reconstruction at step 10 with 200 mAs is shown.

each consisting of m pixels. The matrix $\mathbf{A} \in \mathbf{R}^{pm \times n}$ is the discretization of a line integral operator defined by the X-ray geometry. Solving (1) means reconstructing the volume. Since this inverse problem is ill-posed, it is also important to consider additional information. Other groups have shown, that TV-regularization leads to a better signal to noise ratio and to a reduction of streaking artifacts [4], [5], but one may ask, whether small structures are better recognizable. With TV-regularization the linear equation becomes a convex optimization problem of the form

$$\min_{\mathbf{x}} f(\mathbf{x}) := \|\mathbf{A}\mathbf{x} - \mathbf{y}\|_2^2 + \lambda TV(\mathbf{x}) . \quad (2)$$

For feasibility reasons, we use a differentiable approximation of the total variation $TV(\mathbf{x})$ which is defined as

$$TV(\mathbf{x}) := \sum_{ijk} \sqrt{d(x_{i,j,k}) + \beta^2} \quad (3)$$

with a small $\beta > 0$ and

$$d(x_{i,j,k}) := (x_{i-1,j,k} - x_{i,j,k})^2 + \quad (4)$$

$$(x_{i,j-1,k} - x_{i,j,k})^2 + \quad (5)$$

$$(x_{i,j,k-1} - x_{i,j,k})^2 \quad (6)$$

where the indices i, j and k denote the position in the 3D volume. In [6] the iterative Barzilai-Borwein (BB) solver was successfully used for reconstruction of low-dose cone-beam computed tomography (CBCT) images, delivering good results after just a few (12-30) iterations.

II. MATERIALS AND METHODS

A. Tomosynthesis System

The system that we used for our reconstructions is a Siemens Mammomat Inspiration. Its X-ray source moves with an angular range of maximal 50° and under our operating conditions between -24.82° and $+21.14^\circ$. During this process the system exposes 25 projection images with a size of about 2400×3600 pixels and a pixel spacing of 0.085×0.085 [mm]. The rotation center is at 4.7 cm above the detector and the distance between the x-tube and the detector is about 66 cm [7]. We evaluate one series with 30 peak kilovoltage (kVp) and an overall exposure of 200 mAs (8 mAs per projection), which is higher than the system's automatic mode with an exposure

value defined at 105 mAs for 30 kVp for the mammography phantom.

B. Reconstruction Method

The volume, that we reconstruct, is a box with about $2400 \times 3600 \times 47$ voxels and a voxel size of $0.085 \times 0.085 \times 1 \text{ mm}^3$. It is located close upon the detector and contains the whole phantom. To avoid artifacts and minimize the memory required, our volume is defined exclusively by voxels that are projected into regions of the phantom. Exterior voxels are set to 0.

We applied the algorithm by Barzilai and Borwein, which is based on a Quasi-Newton-Method [8]. Thereby an iteration step has the form $\mathbf{x}_{n+1} = \mathbf{x}_n - \mathbf{H}_n^{-1} \nabla f(\mathbf{x}_n)$ where \mathbf{H}_n is an approximation to the Hessian of $f(\mathbf{x})$. Barzilai and Borwein set $\mathbf{H}_n^{-1} = \alpha_n \mathbf{I}$ where α_n is given by

$$\alpha_n = \frac{(\mathbf{x}_n - \mathbf{x}_{n-1})^T (\nabla f(\mathbf{x}_n) - \nabla f(\mathbf{x}_{n-1}))}{(\mathbf{x}_n - \mathbf{x}_{n-1})^T (\mathbf{x}_n - \mathbf{x}_{n-1})} \quad (7)$$

minimizing $\|(\mathbf{x}_k - \mathbf{x}_{k-1}) - \alpha_n (\nabla f(\mathbf{x}_k) - \nabla f(\mathbf{x}_{k-1}))\|$.

Since the total variation is not differentiable as a function of \mathbf{x} , we use the differentiable approximation $TV(\mathbf{x})$ as defined in (3). Then, the iteration step becomes

$$\mathbf{x}_{n+1} = \mathbf{x}_n - \alpha_n (2 \mathbf{A}^T (\mathbf{A}\mathbf{x} - \mathbf{y}) + \lambda \nabla (TV(\mathbf{x}))) . \quad (8)$$

The influence of TV on the reconstruction process can be managed by the regularization constant λ in (2) and (8) respectively. To speed up the reconstruction process forward and back projection (\mathbf{A} and \mathbf{A}^T , respectively) are written as shaders running on the graphics processing unit (GPU), see [9].

C. Quart Phantom

To evaluate the quality of our reconstructions we used a new mammography phantom, the Quart Mam/Digi phantom [10]. The most interesting features for our reconstruction are the so-called Landolt rings (see Fig. 1,2). These are special rings with a gap in one of the four directions: right, left, bottom or top. The phantom has 12 steps with increasing densities and each step contains a group of six LRs with diameters from $800 \mu\text{m}$ down to $260 \mu\text{m}$.

Fig. 1 shows a projection image of the Quart Mam/Digi phantom. A detailed reconstruction of a group of Landolt rings is depicted in Fig. 2. Furthermore, in the latter the identical region from the Siemens Mammomat Inspiration reconstruction is given. The more LRs are detected correctly in a reconstruction, the better the image quality is. For a fast and objective evaluation we implemented a fully automatic LR detection algorithm based on standardized 12-bit DICOM input datasets.

D. Automatic Landolt Ring Detection

Fig. 3(a) shows a schematic representation of a LR. To measure the detection quality of a LR, three features are calculated (see also Fig. 3(b)):



Fig. 3. (a) LR with gap on the right side. (b) Marked features: center of ring (dot), path inside the ring (line), path in the gap (dotted line) and circle-path outside (line). (c) LRs on Step 7, Exposure 99 mAs, Barzilai Borwein reconstruction, TV $\lambda = 0.5$. (d) Visual output of the automatic LR detection for the first Ring in (c): center, ring and gap are marked correctly. (e) Values on the circle-path through the ring and the gap: the highest peak belongs to the gap.

- 1) Contrast c , based on the gray value v_1 at the center, the mean value v_2 of the intensities along a circular path on the ring and the mean value v_3 on the circle-path outside: $c = ((v_1 - v_2) + (v_3 - v_2))/2$,
- 2) Standard deviation sd of the ring values,
- 3) Difference d between mean gap value and mean ring value.

The calculations are performed with sub-pixel accuracy using bilinear interpolation. The positions of the 12 groups of LRs in the phantom are fix. In order to ensure a more flexible usability of the detection method, offset jumps from an automatically detected landmark to the LR groups are used. Caused by small inaccuracies in the landmark detection, a small search window of $0.5 \times 0.5 \times 1.0 \text{ mm}^3$ for searching the center of the first LR of a group is used - this ensures that the first ring of a group can be determined correctly. A ring is marked at the position where the sum

$$D = \omega_1 c + \omega_2 sd + \omega_3 d, \text{ with } \omega = (\omega_1, \omega_2, \omega_3) = (3, -1, 1) \quad (9)$$

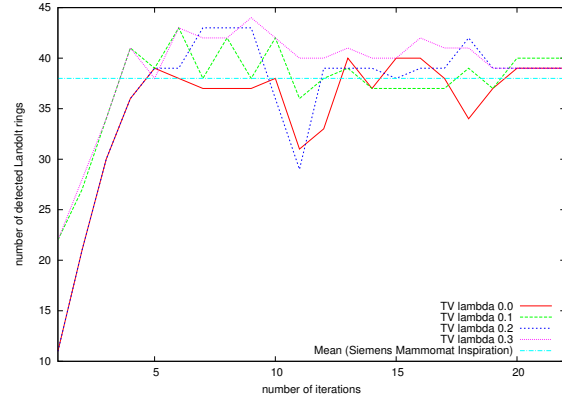
is maximized, varying the center of the LR and the position of the gap. ω was heuristically defined. A ring is counted as detected if the detection sum D is greater than a threshold κ and the attitude of the gap is correctly detected. Suitable values for the detection threshold κ can be chosen taking the density range of the reconstructed DICOM datasets into account. The correct gap positions are known a priori for all LRs of the phantom.

III. RESULTS

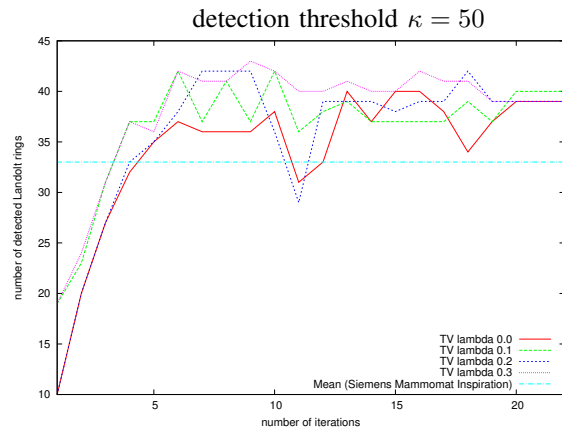
We assign 0.0, 0.1, 0.2, 0.3, 1.0 and 10.0 to the TV regularization constant λ and compare the reconstructions using up to 22 iteration steps. The Landolt ring detection threshold κ is varied to control its influence on the detection rates.

Fig. 4 shows some volume statistics for assigned λ values ($0, 10^{-1}, 10^0, 10^1$). On the left side (a) the residual norm $\|y - Ax\|_2$ is plotted versus the iteration number, whereas on the right side the total variation $\|x\|_{TV}$ of the volume is shown. As one expects, the figure shows decreasing residual norms in (a) and simultaneously increasing total variations of the volumes in (b) with respect to the regularization parameter. Already after 20 iteration steps the desired regularization characteristics are achieved. The differences within the volume statistics for $\lambda \in [0.1, 0.3]$ are marginal. Thus they are omitted in Fig. 4.

Fig. 5 shows the LR detection results for assigned λ values ($\lambda = 0.0, 0.1, 0.2, 0.3$). Two different LR detection thresholds κ were used to define a correct ring count $D > \kappa$ (see (9)): in Fig. 5 (a) $\kappa = 50$ and in (b) $\kappa = 75$. For a higher detection threshold κ less rings were detected e.g. 33 instead of 38 for the Siemens reconstruction. Our results seem to be nonsensitive to threshold variations, because of the higher contrast of our volumes. Both shapes of our data profiles look nearly identical.



(a) LR



(b) LR

Fig. 5. LR counts for TV reconstructions with different λ values. In comparison to the Siemens reconstruction $\lambda = 0.1, 0.2, 0.3$ values mostly deliver higher LR counts after 4 iterations.

The computer used for reconstruction had an Intel Core i7 CPU with 2.97 GHz clock speed and 12 GB RAM. We used a 64-bit Windows 7 OS; the GPU is a NVIDIA GeForce

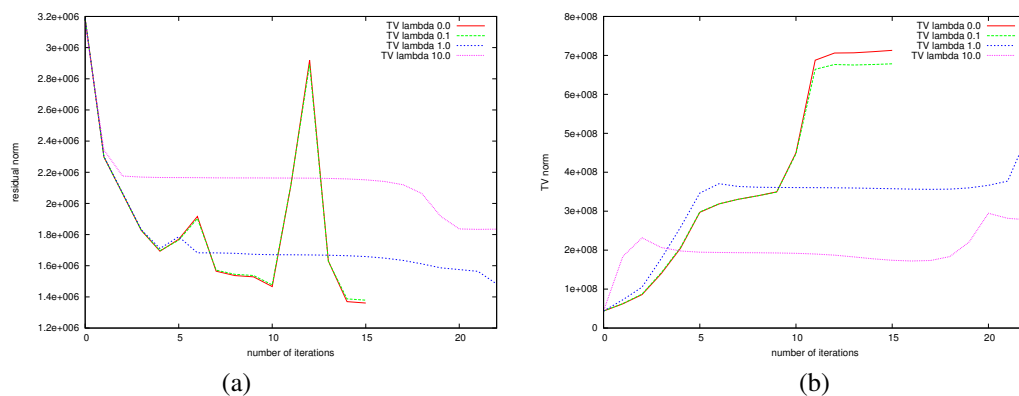


Fig. 4. Iterative reconstruction characteristics for different TV regularization values $\lambda = 0, 10^{-1}, 10^0, 10^1$: (a) residual norm $\|y - Ax\|_2$ and (b) TV norm $\|x\|_{TV}$.

GTX 280. The reconstruction program is compiled as an 32-bit application. Intermediate reconstruction volumes needed during the reconstruction process had to be stored on the hard disk, because of the large size of the Quart Mam/Digi phantom. The runtime for one iteration was approx. one up to two minutes.

IV. DISCUSSION

We showed in this paper that the Landolt ring component of the specific phantom is an adequate tool for the evaluation of DBT algorithms with respect to the representation of small dense structures. TV regularization yielded better perceptibility of the LRs contained in the Quart Mam/Digi phantom, when the parameter λ is adjusted carefully. With the correct iteration number we find more rings, than the reconstruction provided by the manufacturer. A possible explanation for this is a lower standard deviation sd of the values on the ring and thus less noise for comparable contrast values, when using the non-linear TV-regularization.

The following additional steps are planned as future research. We will systematically evaluate our reconstructions for more than 20 iterations over the whole exposure range and time. Investigation and possibly modification of other regularization methods e.g. the L1 norm are planned. With ongoing improvement of the algorithm the required radiation dose could possibly be further reduced.

We will compare the results of the automatic LR detection with the reading of radiologists to evaluate reconstruction quality in a clinical context. Furthermore, we hope that our method can be applied in the context of limited angle breast tomography in order to improve the detection of clinical pathologies (e.g. microcalcifications).

V. CONCLUSION

We conclude that our iterative TV-regularized reconstruction method can be almost optimally adapted to improve the depiction of small clearly defined contrast features in limited-angle cone-beam reconstruction problems.

ACKNOWLEDGMENT

The authors would like to thank the company Quart GmbH for giving us the opportunity to work with the Mam/Digi phantom as well as Dr. Jochen Schenk from the Radiology Institute Hohenzollernstraße of Koblenz for making available the Siemens Mammomat Inspiration system.

REFERENCES

- [1] M. A. Helvie, "Digital mammography imaging: breast tomosynthesis and advanced applications," *Radiologic clinics of North America*, vol. 48, no. 5, pp. 917–929, 2010.
- [2] E. Y. Sidky, X. Pan, I. S. Reiser, R. M. Nishikawa, R. H. Moore, and D. B. Kopans, "Enhanced imaging of microcalcifications in digital breast tomosynthesis through improved image-reconstruction algorithms," *Medical Physics*, vol. 36, no. 11, p. 4920, 2009.
- [3] S. Fränkel, K. Wunder, U. Heil, D. Gross, R. Schulze, U. Schwanecke, C. Düber, E. Schömer, and O. Weinheimer, "Influence of total variation regularization on the representation of small structures in digital breast tomosynthesis - a phantom study," 2013, accepted for "Bildverarbeitung für die Medizin".
- [4] I. Kastanis, S. Arridge, A. Stewart, S. Gunn, C. Ullberg, and T. Francke, "3d digital breast tomosynthesis using total variation regularization," in *Proceedings of the 9th international workshop on Digital Mammography*, ser. IWDM '08. Berlin, Heidelberg: Springer-Verlag, 2008, pp. 621–627.
- [5] E. Sidky, Y. Duchin, I. Reiser, C. Ullberg, and X. Pan, "Optimizing algorithm parameters based on a model observer detection task for image reconstruction in digital breast tomosynthesis," in *NSSMIC, IEEE*, 2011, pp. 4230 – 4232.
- [6] J. C. Park, B. Song, J. S. Kim, S. H. Park, H. K. Kim, Z. Liu, T. S. Suh, and W. Y. Song, "Fast compressed sensing-based cbct reconstruction using barzilai-borwein formulation for application to on-line igr," *Med Phys*, vol. 39, no. 3, pp. 1207–1217, 2012.
- [7] T. Mertelmeier, J. Speitel, and C. Frumento, "3d breast tomosynthesis - intelligent technology for clear clinical benefits," Siemens, Henkestrasse 127, DE-91052 Erlangen, Germany, White Paper A91XP-30011-25C1-7600, 2012, also available as http://www.medical.siemens.com/siemens/en_GLOBAL/gg_sps_FBAs/files/apps/be_sure/3D_breast_tomosynthesis-intelligent_technology_or_clear_clinical_benefits.pdf.
- [8] J. Barzilai and J. M. Borwein, "Two-point step size gradient methods," *Journal of Numerical Analysis*, vol. 8, pp. 141–148, 1988.
- [9] D. Gross, U. Heil, R. Schulze, E. Schömer, and U. Schwanecke, "Gpu-based volume reconstruction from very few arbitrarily aligned x-ray images," *SIAM J. Scientific Computing*, vol. 31, no. 6, pp. 4204–4221, 2009.
- [10] Quart mam/digi website. QUART Medizintechnische Geräte GmbH, Kirchenweg 7, DE-85604 Zorneding, Germany. [Online]. Available: <http://quart.de/en/test-phantoms/mammography.html>